Plasmonics (2007) 2:15–22
DOI 10.1007/s11468-006-9020-9

Optimization of Nanoparticle Size for Plasmonic Enhancement of Fluorescence

Ondrej Stranik · Robert Nooney · Colette McDonagh · Brian D. MacCraith

Received: 27 June 2006 / Accepted: 14 November 2006 / Published online: 29 December 2006

Abstract This paper reports on the enhancement of fluorescence that can result from the proximity of fluorophores to metallic nanoparticles (NPs). This plasmonic enhancement, which is a result of the localized surface plasmon resonance at the metal surface, can be exploited to improve the signal obtained from optical biochips and thereby lower the limits of detection. There are two distinct enhancement effects: an increase in the excitation of the fluorophore and an increase in its quantum efficiency. This study focuses on the first of these effects where the maximum enhancement occurs when the NP plasmon resonance wavelength coincides with the fluorophore absorption band. In this case, the excitation enhancement is proportional to the square of the amplitude of the electric field. The scale of the enhancement depends on many parameters, such as NP size and shape, metal type, and NP–fluorophore separation. A model system consisting of spherical gold/silver alloy NPs, surrounded by a silica spacer shell, to which is attached a fluorescent ruthenium dye, was chosen and the dependence of the fluorescence enhancement on NP diameter was investigated. Theoretical calculations, based on Mie theory, were carried out to predict the maximum possible enhancement factor for spherical NPs with a fixed composition and a range of diameters. Spherical NPs of the same composition were fabricated by chemical preparation techniques. The NPs were coated with a thin silica shell to overcome quenching effects and the dye was attached to the shell.

Key words Plasmonic · Fluorescence enhancement · Metallic nanoparticles

O. Stranik · R. Nooney · C. McDonagh (✉) · B. D. MacCraith
School of Physical Sciences, Biomedical Diagnostics Institute,
Dublin City University,
Dublin 9, Ireland
e-mail: colette.mcdonagh@dcu.ie

Introduction

There is increasing interest in fluorescence-based array sensors (biochips) for biomedical applications. While fluorescence detection offers high sensitivity, there is generally a low level of fluorescence from the biochip due to a monolayer of fluorescent labels, hence the importance of enhancing the fluorescence. This work exploits the enhancement obtained when fluorophores are in the vicinity of metal nanoparticles (NPs) or nanostructures [1–3, 17, 18]. This plasmonic effect is due to the localized surface plasmon resonance (LSPR) at the surface of the metal NP. The LSPR modifies the intensity of the electromagnetic (EM) field around the fluorophore, and this can lead to an increase in the emitted fluorescence intensity. The effect is dependent on many parameters such as metal type, NP size and shape, NP–fluorophore separation, and fluorophore quantum efficiency. There are two possible enhancement effects: an increase in the excitation of the dye and an increase in the quantum efficiency of the dye. The first effect occurs because the excitation rate is directly proportional to the square of the electric field amplitude, and the maximum enhancement occurs when the NP plasmon resonance wavelength coincides with the dye absorption band [4]. The second effect involves an increase in the quantum efficiency of the dye and is maximized when the NP resonance wavelength coincides with the dye emission band [5]. This paper focuses on the first effect, excitation enhancement. We report the enhancement of fluorescence of a dye that has been immobilized on the surface of a spherical metal NP, and the dependence of the fluorescence on NP diameter. Our model system consists of spherical gold/silver alloy NPs, surrounded by a silica spacer shell, to which is attached the fluorescent dye. A ruthenium dye complex was chosen in our experiments due to its strong absorption, high quantum efficiency, and the

large Stokes shift. The enhanced fluorescence is measured in solution and the dependence on NP diameter is investigated. Theoretical calculations were carried out to predict the maximum enhancement factor. Spherical gold/silver alloy NPs with a fixed composition were fabricated with a range of diameters by chemical preparation techniques. The NPs were coated with a thin silica shell (approximately ~5 nm) to minimize metal-fluorophore quenching effects, and the dye was ionically attached to the shell. Experimental fluorescence enhancement factors were measured and compared to the theoretical model.

Theory

The EM theory that describes the fluorescence emission of a dye in the vicinity of a NP can be considered in three stages. The first stage is the interaction of the excitation light with the NP. The second stage is the interaction of the altered EM field in the vicinity of the NP with the dye, and the third interaction is that of the dye fluorescence with the NP. The interaction of an EM wave with a spherical particle has been solved exactly by Mie [6]. This theory predicts the distribution of the EM waves both outside and inside the particle, when the particle is illuminated by a plane wave. From these results, extinction coefficients as a function of illumination wavelength and scattering coefficients as a function of angle can be predicted. The theory also predicts that, if the particle is sufficiently small (in the nanometer range) and if the material of the NP has a negative dielectric constant (as in the case of metals), there will be a resonance between the illuminating light and the NP, which results in an increase of extinction coefficient for this wavelength range. This constitutes the LSPR effect.

To mathematically formulate this problem, we consider a system consisting of a gold/silver NP of radius r, with a silica shell coating (of thickness d), placed at the origin of a coordinate system ($\mathbf{e}_x$, $\mathbf{e}_y$, $\mathbf{e}_z$) (vectors are denoted by bold font) and with an incident plane wave with x-polarization and wavelength propagating in the z-direction. The electric field of the incident wave is expressed as

$$\mathbf{E}_i(r,\theta,\phi) = E_0 \exp(irk\ \cos\phi)\mathbf{e}_x \tag{1}$$

where $k=2\pi/\lambda$. The interaction of the field with the NP creates an additional field $\mathbf{E}_s$, which is superimposed on the incident field outside the sphere. $\mathbf{E}_s$ is expressed as

$$\mathbf{E}_s(r,\theta,\phi) = E_0 \sum_{n=1}^{\infty} i^n \frac{2n+1}{n(n+1)} (ia_n \mathbf{N}_{e1n} - b_n \mathbf{M}_{o1n}) \tag{2}$$

where $\mathbf{N}_{e1n}$ and $\mathbf{M}_{o1n}$ are vector spherical harmonics and a_n and b_n are scattering coefficients [7]. Only the refractive indices of the NP (n_{np}), shell (n_{SiO2}), and embedded medium (n_{H2O}) are required for this calculation. Values of $n_{SiO2}=1.5$ and $n_{H2O}=1.33$ were assumed and, for simplicity, their wavelength dependence was not taken into account. The refractive index of an alloy NP with molar ratio of x_{Au} was obtained from a model, which was similar to that used in reference [8], except that, in this case, the contribution of s-electrons was described using the classical Drude treatment. This model was based on a combination of the dielectric properties of gold and silver. Knowing the exact distribution of the electric field, an extinction cross section can be derived [7]. The expression for the cross section is shown in Eq. 3. This calculated extinction cross section can be compared with data measured via absorption spectroscopy.

$$C_{ext} = \frac{2\pi}{k^2} \sum_{n=1}^{\infty} (2n+1)\mathrm{Re}\{a_n + b_n\} \tag{3}$$

The excitation rate of a fluorescent dye depends linearly on the intensity of the excitation light in the direction of the absorption dipole, $\mathbf{e}_d$, of the molecule (for simplicity, the molecule is approximated to a single dipole). When the dye molecule is placed in the proximity of the NP, the electric field acting on the dipole changes from $\mathbf{E}_i$ to $\mathbf{E}_i+\mathbf{E}_s$. Therefore, we can define the excitation enhancement factor, f_{enh}, for one dye molecule as a ratio of intensities:

$$f_{enh}(r,\theta,\phi) = \frac{|(\mathbf{E}_i + \mathbf{E}_s)\mathbf{e}_d|^2}{|\mathbf{E}_i \mathbf{e}_d|^2} \tag{4}$$

The orientation of a dye molecule at the surface of a NP has a significant influence on the enhancement factor. The electric field at the surface of a silica shell coated on the NP is almost perpendicular. It follows from this and from Eq. 4 that molecules, which are oriented normally, are considerably more excited than those oriented tangential to the surface. In our model, we assume that the dipole orientation at the NP surface is random. The average intensity over all possible dipole positions due to an EM field E is given by 1/3 $|E|^2$. Therefore, the averaged enhancement factor can be written as:

$$f_{enh}(r,\theta,\phi) = \frac{|\mathbf{E}_i + \mathbf{E}_s|^2}{E_0^2} \tag{5}$$

In our experimental measurement, we detected fluorescence from dye molecules distributed uniformly over the silica shell. Hence, the enhancement was averaged over all possible positions. This is given by

$$F_{enh}^a = \frac{1}{4\pi E_0^2} \int_0^{2\pi} \int_0^{\pi} |\mathbf{E}_i(a+d,\theta,\phi) + \mathbf{E}_s(a+d,\theta,\phi)|^2 \sin(\theta) d\theta d\phi \tag{6}$$

where d and a are the shell thickness and NP radius, respectively. Due to the spherical symmetry, the enhance-

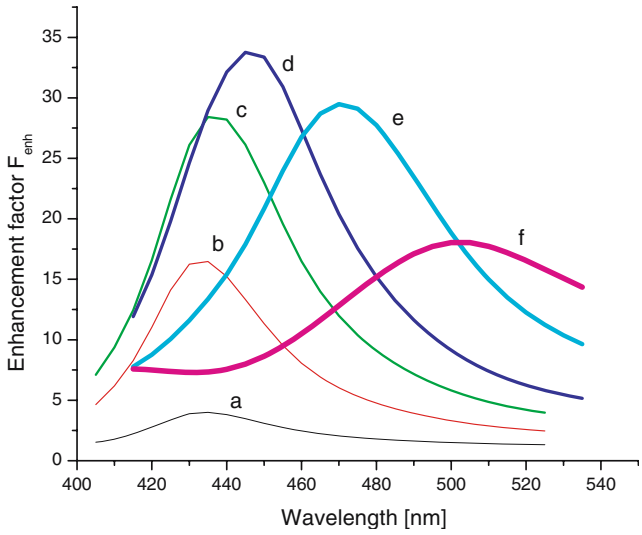

Figure 1. Dependence of the enhancement factor F^a_{enh} on the excitation wavelength for different NP sizes. Parameters: gold/silver molar ratio x=0.2, thickness of the silica shell d=5 nm. Radius of the NPs *a* 5 nm, *b* 10 nm, *c* 15 nm, *d* 20 nm, *e* 30 nm, *f* 40 nm.

ment factors are also valid for illumination of the sphere with unpolarized light.

The emission of the dye is altered as well. The fluorescence does not increase if the quantum efficiency of the dye is high and if the plasmon resonance does not coincide with the emission wavelength. However, the quantum efficiency of the dye can decrease due to the nonradiative de-excitation resulting from dye–NP proximity [9]. For this reason, the dyes were not attached directly onto the NP but a silica shell of 5-nm thickness was added. At such distances, the excitation enhancement is still significant and should overcome the negative effect of the quenching, which is much less than at zero distance [1, 19, 20]. Therefore, the numerically calculated excitation enhancement F^a_{enh} is the maximum enhancement of the fluorescence for this system, and, depending on the strength of the quenching, the experimentally measured enhancement will be decreased. The results of the theoretical calculations of the maximum enhancement factors are given in "Results and discussion" and are compared with the experimentally measured values.

Materials and methods

Materials

(3-amino propyl)trimethoxysilane (APTS), sodium silicate solution [$Na_2O(SiO_2)_{3-5}$, 27 wt.% SiO_2], hydrogen tetrachloroaurate ($HAuCl_4$), silver nitrate (AgNO3), sodium citrate, sodium borohydride, and L ascorbic acid were all purchased from Sigma Aldrich. Deionized water >18 MΩ was used from a Millipore Academic system. All glassware was cleaned with an aqua regia solution prior to synthesis. Ruthenium (II) tris (4,7 diphenyl-1,10 phenanthroline dichloride) [abbreviated to $Ru(dpp)_3^{2+}$] was prepared as in [10]. The dye has a broad absorption peak ranging from 410 to 590 nm. The dye has a large Stoke's shift with the emission peak at 620 nm (see Figure 7). Its intrinsic fluorescence lifetime is in the range of microseconds and the quantum efficiency is around 0.5.

Synthesis of gold/silver NPs

Gold/silver alloy NPs with four different radii were synthesized. The smallest (13 nm radius) NP was prepared in aqueous solution by the coreduction of silver nitrate and chloroauric acid with sodium citrate [11, 12]. In this method, 2 ml of 1 wt.% sodium citrate was added dropwise with rapid stirring to a boiling solution of silver nitrate (20.3 mmol) and chloroauric acid (5.08 mmol) dissolved in 95 ml of deionized water. The solution was stirred for a further 30 min, in which time the solution changed from a light blue to a light red to a dark yellow color. The final concentration of colloid was 3.2×10^{10} particles per milliliter with a molar ratio of four silver atoms to every gold and a NP radius of 13 nm.

The three larger-diameter NPs were synthesized using a seeded growth method whereby a seed solution containing the 13-nm-radius NP synthesized above was added with sodium citrate to an aqueous solution of chloroauric acid and silver nitrate [13]. The reduced gold atoms precipitate onto the NPs in preference to the formation of new nucleating sites, thereby increasing the size of the NP seeds. For this procedure, 75 ml of boiling silver/gold seed NPs from the above procedure and 2.5 ml of 1 wt.% sodium citrate was

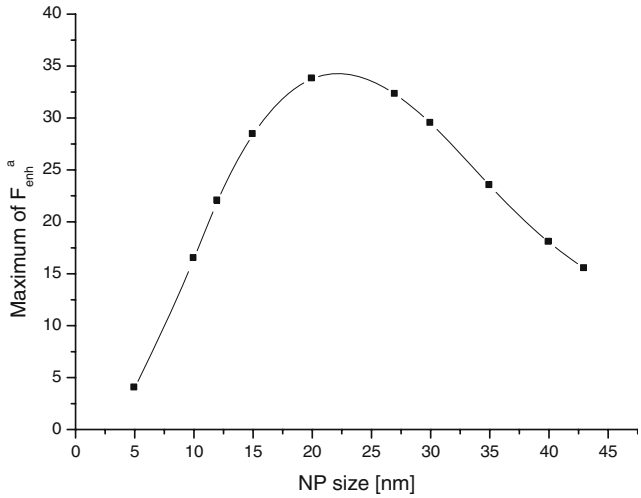

Figure 2. Dependence of the maximum enhancement on the NP size. Parameters: gold/silver molar ratio x=0.2, thickness of the silica shell d=5 nm.

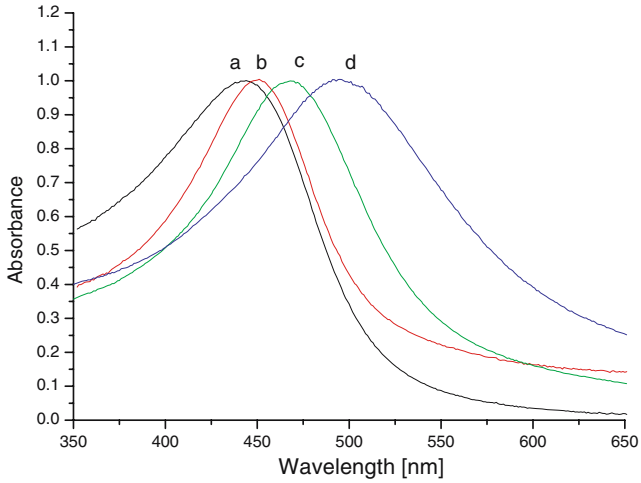

Figure 3. Optical extinction spectra of the gold/silver NPs (*a* 13 nm, *b* 27 nm, *c* 36 nm, *d* 40 nm).

added simultaneously and with rapid stirring to a boiling solution of 23.5 mmol silver nitrate and 5.88 mmol chloroauric acid dissolved in 75 ml of deionized water. The solution was stirred for a further 30 min, during which the solution darkens slightly in color. The final concentration of colloid was 1.6×10^{10} particles per milliliter with a molar ratio of four silver atoms to every gold and a particle radius of 27 nm. This procedure was repeated a further two times using the NPs from the previous synthesis to generate gold/silver alloy NPs with average radii of 36 and 40 nm.

Synthesis of the silica shell around the NPs

NPs were coated with a silica shell by precipitation from a sodium silicate solution [14]. An aqueous solution of 0.5 ml of 1 mM was added to 100 ml of each NP sol under vigorous stirring and allowed to stand for a further 30 min to ensure attachment of the APTS ligand to the surface of the NPs. Separately, a solution of activated silica was prepared by lowering the pH of a 0.54-wt.% sodium silicate solution to 10.5 with progressive additions of the cationic exchange resin. Finally, 4 ml of the activated silica solution was added to the NP solution with vigorous stirring and allowed to stand for a further 24 h. Shell thicknesses of 5 nm were achieved using this method.

Synthesis of the silica NPs

Monodispersed silica NPs were prepared using a microemulsion method [15]. The radius of the silica NPs was 30 nm. NPs were redispersed in deonized water to a concentration matching that of gold–silver alloys.

Attachment of ruthenium dye complex to silica-coated NPs

A monolayer of the dye $Ru(dpp)_3^{2+}$ was attached electrostatically to the outer silica layer of the NPs. At pH 7, which was used in all the experiments, the silica coating on the NP is negatively charged in aqueous solution. On the

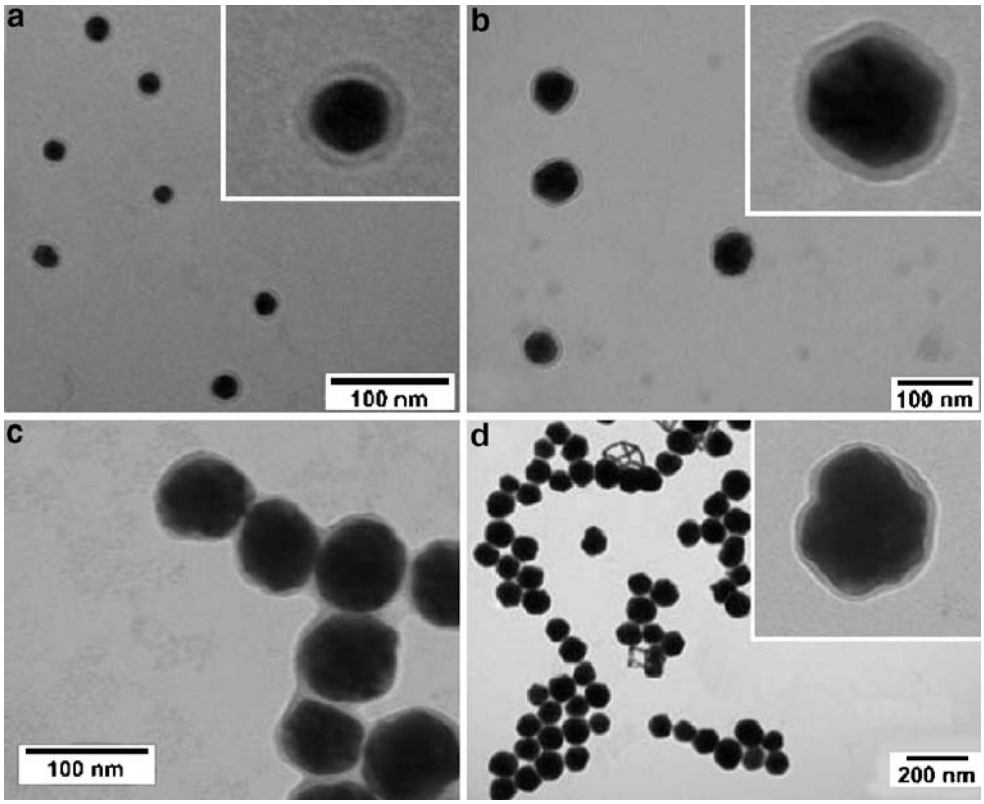

Figure 4. TEM images of gold/silver NPs (**a** sample 1, **b** sample 2, **c** sample 3, **d** sample 4).

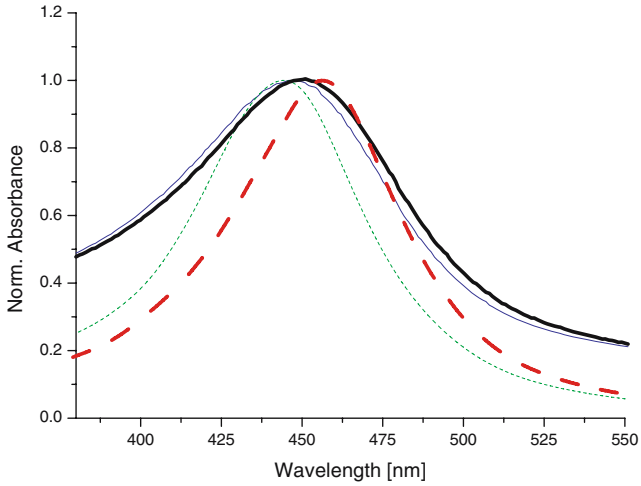

Figure 5. Experimental (*solid line*) and theoretical (*dashed line*) optical extinction spectra of the NP with radius 27 nm with (*thick line*) or without 5-nm silica shell (sample 2).

other hand, the dye has a positive charge in solution. When the dye is added to the solution of NPs, due to electrostatic interactions, the dye formed an ionic bond with the surface of the silica shells.

Characterization techniques

The UV-visible extinction spectra of the NPs in water solution were measured with a Cary 50 Scan UV-Visible Spectrophotometer (Varian) in transmission mode. TEM micrographs were obtained using a Hitachi 7000 TEM operated at 100 kV. Images were captured digitally using a Megaview 2 CCD camera. Specimens were prepared by dropping aqueous solutions onto formvar carbon coated copper grids.

Protocol for normalized fluorescence measurement

The fluorescence enhancement is measured by comparing the signal from the NP–dye system to that of the equivalent dye concentration without the NPs. Firstly, the optimum concentration of NPs in solution must be chosen to take account of inner filter effects [16], which are caused by the strong absorption of the NPs. If the NP concentration is too high, the intensity of illumination rapidly decreases throughout the sample, which makes it impossible to compare to the solution without NPs. On the other hand, too low a concentration of the NPs would mean too low a concentration of the dye, which would be undetectable. Hence, an optimum NP dilution was established empirically based on the two limiting situations discussed above. This optimum dilution corresponds to an absorbance of the NP solution in a 1-cm cuvette of approximately 0.3. The resulting concentration of NPs in solution was about 3×10^{9} particles per milliliter. Next, the dye concentration required to form a monolayer on the NP surface was estimated from the concentration of colloids and from the geometrical size of the dye to be 10^{-7} M. The reference solution used was a 10^{-5}-M solution of the dye in ethanol because the dye is not very soluble in water at high concentration. Self-quenching of the dye was not expected because of the large Stokes shift. The details of the fluorescence measurement are as follows: 1 ml of the NP solution, for each NP diameter, and 1 ml of deionized water were stored in ependorf tubes. Ten microliters of 10^{-5} M ruthenium dye standard was added to the tubes. Aliquots of 100 μl were placed in black microplate wells and the fluorescence was measured with a Safire (Tecan) microplate reader. For the NP–dye and pure dye solutions, the excitation wavelength matched both the LSPR of the NPs and the absorption band of the dye.

Results and discussions

Results of theoretical calculations

As indicated in "Materials and Methods," a fixed gold molar ratio, x_{Au}, of the alloy was chosen for all NPs and the theory was developed for this concentration. Because the gold concentration in the alloy NP will affect the LSPR wavelength and hence the enhancement factor, x_{Au} was chosen such that the LSPR wavelengths for all NP radii would overlap the ruthenium dye absorption band. This is feasible as the absorption band is quite broad, ranging from 410 to 590 nm (as can be seen from Figure 7). To achieve this, the optimum x_{Au} was chosen to be 0.2. Figure 1 shows the dependence of the calculated enhancement factor on excitation wavelength for different NP sizes, each surrounded by a silica shell of 5-nm thickness. These data

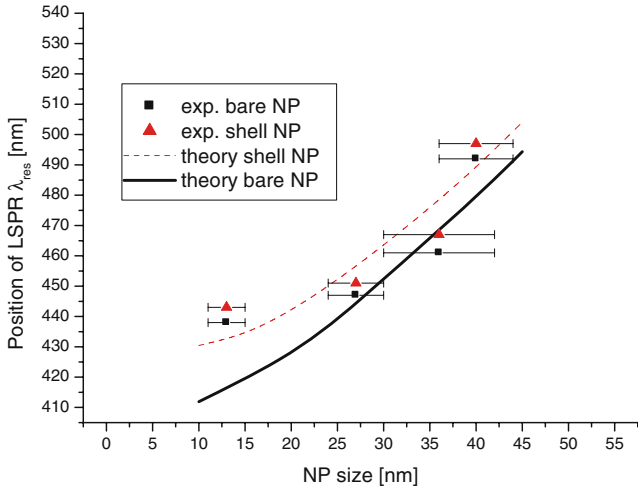

Figure 6. Experimental measured and theoretical predicted maxima of the extinction peaks of NP with or without silica shell (λ_{res}).

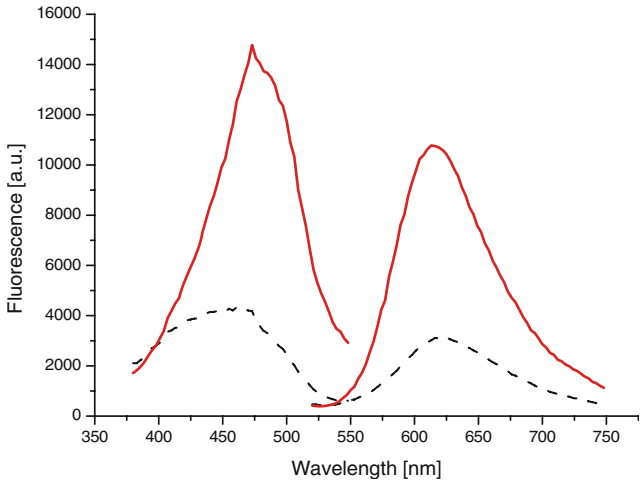

Figure 7. Excitation and emission spectra of the Ru-dye in a water solution (*dashed line*) and in the solution with 27 nm radius NPs (*solid line*) sample 2.

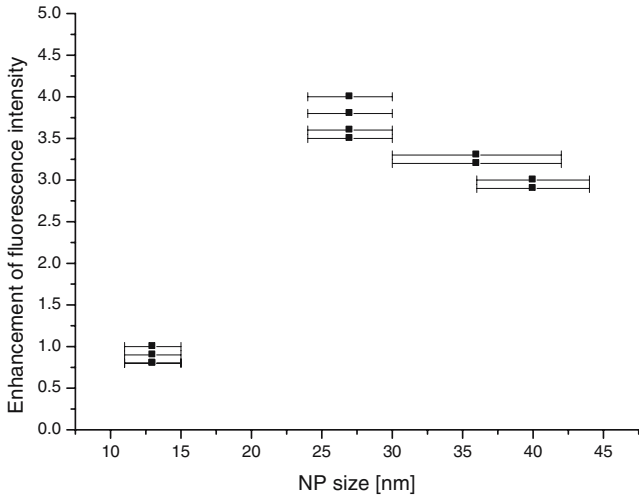

Figure 9. Experimentally measured dependence of the fluorescence enhancement on the size of the NPs.

were calculated numerically from Eq. 6. From these data, it can be seen that for each NP size, there is a maximum wavelength of the enhancement. These curves are not generally identical to the extinction spectra calculated from Eq. 3. In the case of small NPs, the profiles and positions of the extinction spectra and the enhancement factor are similar, but with increasing size, the maximum wavelength for enhancement shifts to longer wavelengths compared to the extinction maxima. From the data in Figure 1, the dependence of the maximum enhancement wavelength with NP radius can be plotted. This is shown in Figure 2 and indicates that maximum fluorescence enhancement should occur for a radius in the region of 20–25 nm. This dependence on NP size is explained as follows: if the NP is much smaller than the illumination wavelength, the E-field amplitude on the surface does not depend on the NP size and is inversely proportional to the ratio of NP–dye distance and NP radius. This corresponds to the electrostatic approximation. Therefore, for a constant NP–dye distance, the E-field amplitude increases with NP radius up to a point where the electrostatic approximation no longer holds. This is the case for larger NP sizes (radius ~0.1 times the wavelength) where the LSPR effect is weaker and the amplitude of the field decreases.

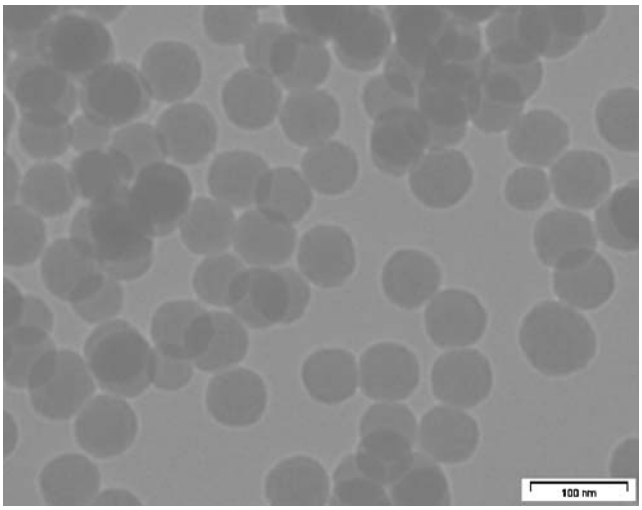

Figure 8. TEM image of silica NPs. Average radius of the NPs is 30 nm.

NP characterization

As described in "Materials and Methods," gold/silver alloy NPs, with x_{Au} of 0.2, with sizes ranging from 13 to 40 nm radius, were synthesized from colloidal solution. The absorption spectra of all NPs were measured and the data are shown in Figure 3. It can be seen that there is a clear LSPR peak for each size of NP and that the peak wavelength shifts to longer wavelengths with increasing size. When the 5-nm silica shell was added to the NPs, a small red shift was observed, as predicted. The presence of this shift helped to confirm the presence of the shell on the NPs. Evidence of this shift can be seen in Figure 6. TEM microscopy was also carried out to determine the exact particle size and shell thickness. A selection of TEM images is shown in Figure 4. These data confirm that the particles are mainly spherical and

Table 1 Sizes of the NPs and thickness of their SiO_2 shells

	Sample 1 (nm)	Sample 2 (nm)	Sample 3 (nm)	Sample 4 (nm)
NP radius	13±2	27±3	36±6	40±4
SiO_2 thickness	4±0.4	4.8±0.7	5.7±0.9	7.8±1.3

that they have the small variation in the size. Average particle size and shell thickness values were measured from these data. Table 1 documents the average NP radius and average shell thickness. Figure 5 shows a comparison of the theoretically computed optical extinction spectrum (also shown in Figure 3) with the experimental optical extinction data for a NP with a radius of 27 nm where the NP dimensions were measured from the TEM data. The experimental spectra are broader due to the small amount of polydispersity present. Computed and experimental data (position of LSPR peak) for all NP sizes are shown in Figure 6. Here, an average shell thickness of 5 nm was assumed for all NPs. Clearly there is quantitative agreement between theory and experiment.

Estimation of fluorescence enhancement factor

The protocol for measurement of the fluorescence enhancement factor was described in "Materials and Methods." Both emission and excitation spectra were measured for (1) the NP–dye combination in solution and (2) the same concentration of dye in solution without the NPs. In these experiments, the excitation spectra were measured at an emission wavelength of 620 nm and the emission was measured for excitation wavelengths corresponding to the maximum in excitation spectra. Figure 7 shows the data for a NP of radius 27 nm. It can be seen from the data that there is an average enhancement factor of 4 in both excitation and emission. The fluorescence enhancement, defined as the ratio between the emission intensity for NP–dye and that of dye alone, has been measured for all NPs and is plotted in Figure 9 as a function of NP radius. From this, it can be seen that the maximum enhancement factor is 4, whereas no enhancement was measured for the smallest NP (radius= 13 nm). The enhancement drops off after a radius of 27 nm.

In a separate experiment we confirmed that the enhancement of the fluorescence was due to the LSPR and that the enhancement factor was not influenced by the attachment of the fluorescent dye to the surface of the silica shell coating the NPs. Prior to the experiment, silica NPs were prepared as described in "Materials and Methods." The size of the silica NPs was chosen to be approximately the same as the size of metal NPs, giving the biggest enhancement (sample 2, radius 27 nm). The silica NPs were analyzed by TEM (see Figure 8) and the diameter of the NPs was determined to be 60 nm. In the next step we repeated the protocol for measurement of the fluorescence enhancement factor (described in "Materials and Methods") where, instead of metal NPs (radius ~27 nm), silica NPs (radius ~30 nm) of the same concentration were used. The recorded fluorescence spectra from the dye attached to the silica NPs and from free dye in solution were almost identical. This indicated that the attachment of the dye to the silica does not influence the emission properties of the dye (quantum efficiency), and therefore, the observed enhancement of the fluorescence from the dye attached to gold silver NPs coated with the silica shell is only due to the LSPR.

Next, the experimental data in Figure 9 were compared with the maximum achievable enhancement values in Figure 2. There is qualitative agreement with respect to the dependence on NP size and the measured enhancement factor is about nine times less than that predicted. This indicates that the induced nonradiative de-excitation rates are still quite significant at the NP–dye distance of 5 nm, leading to the decrease of the quantum efficiency of the dye. Further, from the similar dependence of the enhancement on the NPs' size, it follows that the quenching does not significantly vary with the NP size in the range between 13 and 40 nm. We are aware of the fact that this estimation of the quenching could be also affected by the experimental error if not all the dye binds to the shell. In this case, the unbound dye will not contribute to the enhancement due to the increased separation.

Conclusion

We have studied the influence of metal NPs on the fluorescence properties of a dye in solution, where we focused in particular on the influence of NP size. We compared, theoretically and experimentally, fluorescence from a ruthenium dye in a pure water solution and from the dye of the same concentration attached to the gold/silver NPs with a silica shell. Based on the excitation enhancement of a dye, our mathematical model predicted an optimum size of the NP of around 20–25 nm. Samples of gold/silver alloys with different sizes were successfully prepared and a silica shell of desired thickness was produced. The samples were characterized using absorption spectroscopy and TEM. The optical extinction spectra compared well with those computed theoretically. We experimentally observed the enhancement of fluorescence due to the presence of the NPs in solution, and we measured the dependence of the fluorescence enhancement on the size of the NPs. The biggest enhancement was achieved for NPs with a 27-nm radius, which coincides with the calculated optimum radius. The experimental values of the enhancement were, on average, nine times lower than the theoretically predicted value. This is most likely an indication of the presence of a quenching effect due to dye–NP proximity. The key result of this work is that plasmonic enhancement of fluorescence was observed in this solution-based system and that the optimal NP radius of 27 nm agreed well with that predicted for excitation enhancement. Further work will address the optimal dye–NP separation in an effort to optimize the enhancement factor.

Acknowledgment This material is based on works supported by Science Foundation Ireland under Grant No. 05/CE3/B754.

References

1. Sokolov K, Chumanov G, Cotton TM (1998) Enhancement of molecular fluorescence near the surface of colloidal metal films. Anal Chem 70(18):3898–3905
2. Stich N, Gandhum A, Matushin V et al (2001) Nanofilms and nanoclusters: Energy sources driving fluorophores of biochip bound labels. J Nanosci Nanotechnol 1(4):397–405
3. Lakowicz JR, Malicka J, Gryczynski I et al (2003) Radiative decay engineering: the role of photonic mode density in biotechnology. Anal Biochem 36(14):R240–R249
4. Stranik O, McEvoy HM, McDonagh C et al (2005) Plasmonic enhancement of fluorescence for sensor applications. Sens Actuators B Chem 107(1):148–153
5. Lakowicz JR, Shen B, Gryczynski I (2001) Intrinsic fluorescence from DNA can be enhanced be metallic particles. Biochem Biophys Res Commun 286:875–879
6. Mie G (1908) Beitrage zur Optik trueber Medien speziell kolloidaler Metalloesungen. Ann Phys 25:377–445
7. Bohren CF, Huffman DR (1983) Absorption and scattering of light by small particles. Wiley, New York
8. Gaudry M, Lerme J, Cottancin E et al (2001) Optical properties of (AuxAg1-x)(n) clusters embedded in alumina: evolution with size and stoichiometry. Phys Rev B 64(8):art. no.-085407:1–7
9. Huang T, Murray RW (2002) Quenching of [Ru(bpy)3]2+ fluorescence by binding to Au nanoparticles. Langmuir 18:7077–7081
10. Watts RJ, Crosby GA (1971) Spectroscopic characterization of complexes of ruthenium and iridium with 4,4′-diphenyL2,2′-bipyridine and 4,7-diphenyl-1,lO-phenanthroline. J Am Chem Soc 93:318
11. Link S, Wang ZL, El-Sayed MA (1999) Alloy formation of gold–silver nanoparticles and the dependence of the plasmon absorption on their composition. J Phys Chem B 103(18):3529–3533
12. Turkevich J, Stevenson PC, J Hillier (1951) A study of the nucleation and growth processes in the synthesis of colloidal gold. Discuss Faraday Soc 11:55
13. Brown KR, Walter DG, Natan MJ (2000) Seeding of colloidal Au nanoparticle solutions. 2. Improved control of particle size and shape. Chem Mat 12(2):306–313
14. LizMarzan LM, Giersig M, Mulvaney P (1996) Synthesis of nanosized gold-silica core-shell particles. Langmuir 12(18):4329–4335
15. Santra S, Wang K, Topec R et al (2001) Development of novel dye doped silica nanoparticles for biomarker application. J Biomed Opt 6(2):160–166
16. Rendell D (1987) Fluorescence and phosphorescence. Wiley, New York
17. Wokaun A, Lutz HP, King AP et al (1983) Energy-transfer in surface enhanced luminescence. J Chem Phys 79(1):509–514
18. Weitz DA, Garoff S, Gersten JI et al (1983) The enhancement of Raman-scattering, resonance Raman-scattering, and fluorescence from molecules adsorbed on a rough silver surface. J Chem Phyf 78(9):5324–5338
19. Anger P, Bharadwaj P, Novotny L (2006) Enhancement and quenching of single-molecule fluorescence. Phys Rev Lett 96:113002
20. Mayer C, Stich N, Schalkhammer T et al (2001) Slide-format proteomic biochip based on surface-enhanced nanocluster-resonance. Fresenius J Anal Chem 371:238–245